Interfacial plasticity controls material removal rate during adhesive sliding contact

Kai Zhao [1,2] and Ramin Aghababaei [1,*]

[1]*Surface Mechanics and Tribology Group, Department of Engineering, Aarhus University, 8000 Aarhus C, Denmark*
[2]*Jiangsu Key Laboratory of Advanced Food Manufacturing Equipment and Technology, School of Mechanical Engineering,
Jiangnan University, Wuxi 214122, China*

Adhesive wear is a result of material exchange due to localized adhesive bonding between surface asperities at small scales. It has been recently debated whether a linear wear relation can be observed at the single-asperity level. Using large-scale atomistic simulations, we show that the wear relation is a direct result of the material removal mechanism at the asperity level. In the presence of weak adhesion, sliding is dominated by frictional slipping (i.e., dislocations glide in the contact plane), where occasional atomic cluster detachments and a sublinear wear relation are expected. Alternatively, a linear relation between the volume of detached material and the frictional work can be obtained when bulk plasticity dominants material removal at the asperity tip. Under this condition, high-shear stresses at the contact trigger the migration of misfit dislocations into the asperity bulk, causing severe plastic deformation via dislocation-mediated interface migration. This result highlights that the state of stresses at contact governs the process of material removal and wear relation at the asperity level.

I. INTRODUCTION

Over the past few years, several efforts have been made to understand mechanisms of material detachment and wear at different length scales [1–4]. The fact that the material surface is rough and made of numerous irregular "asperities" [5–9] makes it difficult to establish a unified theory to describe wear across scales. To study wear at the macroscale, one may envisage wear at the multiasperity level as a collective result of isolated wear events occurring at single asperity [10]. Upon the assumption that the friction and wear may originate from the cold welding and plastic deformation of contacting asperities [11], the wear behavior can be empirically described with the well-known Archard's law [12,13]: $V_{\mathrm{wear}} = kNS/H$, where V_{wear} is the wear volume, k is the wear coefficient, N is the applied normal load, S is the sliding distance, and H is the material hardness. Archard argued that this linearity can be recovered at the asperity level by assuming that contacting asperities deform plastically and material detachment occurs by the removal of lumps, and this is independent of the assumed contact model. Assuming that an asperity contact of size a leads to material removal of volume a^3 over a sliding distance of a, one can recover a linear relation between the wear rate (i.e., wear volume per sliding distance) and the asperity contact area, which is also proportional to N/H, considering plastic deformation at the asperity contact.

The development of atomic force microscopy (AFM) [4,14–16] made it possible to access *in situ* information about material transfer at the nanoscale. While some AFM-based wear experiments [17] and molecular dynamics (MD) wear simulations [18] showed that the wear volume correlates linearly with the applied normal load and sliding distance, recent AFM-based studies [2–4] reported nonlinear wear behavior at the nanoscale which cannot be described by the Archard's model. Furthermore, some studies reported the fracture failure of AFM tips during sliding contact [19,20] instead of gradual plastic deformation. These observations further question the origins of wear relations at the asperity level [21]. A similar discussion has been recently made about the emergence of self-affine surface roughness as a result of subsurface plasticity [22] and fracture [8] processes.

Our previous studies [21,23–25] shed a first light to this puzzle by showing a critical length scale that controls the transition from plasticity to fracture in adhesive wear mechanisms at the asperity level. Furthermore, it is found that this critical length controls the tangential (frictional) force (F_T) and sliding distance (S) such that their product, i.e., the tangential work ($\int F_T dS$), is always proportional to the debris volume [26]. This linear relation was first hypothesized by Reye [27] (also referred to as Fleischer's model in the German literature [28]) and intermittently studied experimentally [27,29–31]. In present study we refer to this correlation as Reye's relation, to be distinguished from Archard's relation. To rationalize a linear wear relation at the asperity level, Archard argued that the wear rate (i.e., wear volume per sliding distance) linearly correlates with the contact area, assuming that the material detachment is dominated by plastic deformation [12,13]. Considering the classical Bowden and Tabor hypothesis [11] (i.e., contact area in the case of plastic deformation is proportional to the applied normal load), one can recover a linear correlation between the wear volume and the contact area. Recent studies, however, reported the breakdown of the linear relation between the contact area and the normal load at the nanoscale asperity level [32,33]. This
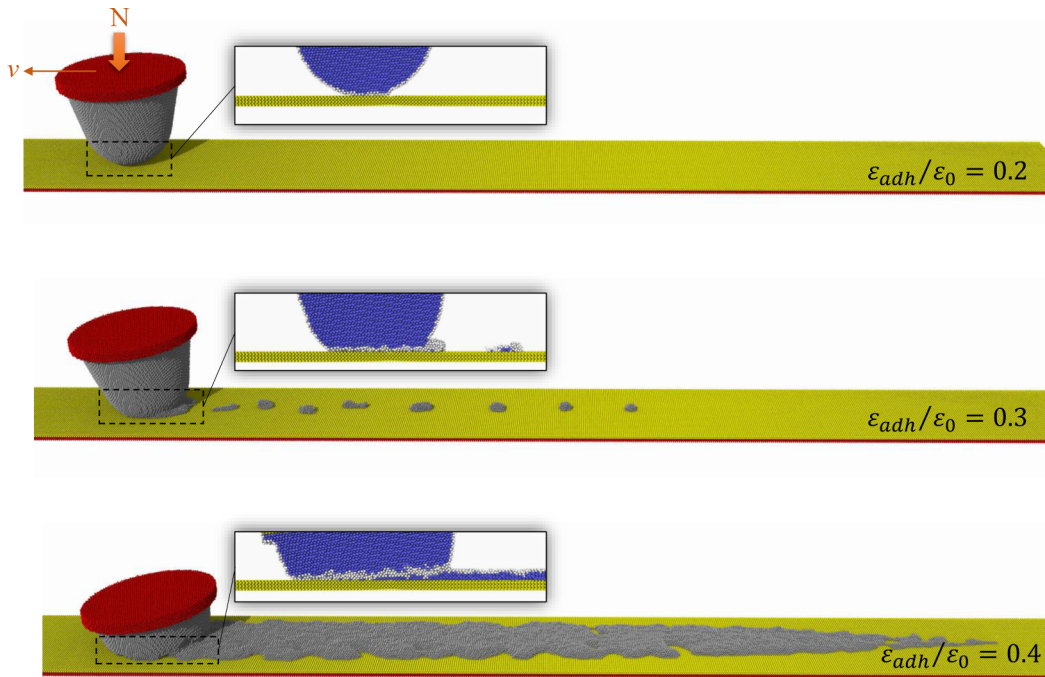
*aghababaei@eng.au.dk

FIG. 1. Snapshots of three MD simulations under different interfacial adhesions. From top to bottom, this figure shows three wear behaviors for different degrees of interfacial adhesion, i.e., (a) frictional sliding (no wear) at $\varepsilon_{adh}/\varepsilon_0 = 0.2$, (b) atomic cluster detachment at $\varepsilon_{adh}/\varepsilon_0 = 0.3$, and (c) continuous material detachment via plastic smoothing at $\varepsilon_{adh}/\varepsilon_0 = 0.4$. A normal force ($N$) is applied on the top layer along the y direction, and a constant velocity (v) is applied on the red top layer along the x direction. Insets demonstrate a detailed atomic structure at the contact between the asperity and the substrate for each simulation. Atoms in the insets are colored by the common neighbor analysis, where the blue and white atoms are of bcc and amorphous structures. Simulations movie can be seen in the Supplemental Material, Movie 1 [34].

breakdown is often explained by the contribution of interfacial adhesion and frictional sliding on the contact area, and consequently, on the friction and wear phenomena at the asperity level [26].

To develop a physics-based adhesive wear model, one needs to understand when and how material transfers between solid surfaces during adhesive sliding contact. Here we perform systematic large-scale MD simulations to study the process of material transfer from an asperity tip during sliding contact over a flat rigid substrate under various adhesion and loading cases. Our results show that the interfacial adhesion controls the mechanism and magnitude of material exchange at the asperity level. Additionally, we show that the Reye's wear relation (i.e., a linear relation between the wear volume and the tangential work) can be recovered at the single-asperity level in a high range of interfacial adhesion, where bulk plasticity dominates the material removal at the asperity tip.

II. SIMULATION SETUP

We study the process of material transfer during adhesive contact by simulating the sliding of a single probe made of Fe over a rigid flat substrate. The AFM probe tip is modeled as a cone shape asperity with the rounded end (see Fig. 1). Since the tip radius R_t [~6.2 nm, see Supplemental Material (SM), Fig. S1 [34]] here is much smaller than the critical length scale of bcc Fe [23], the fracture-induced material removal will be

absent in this study. We set different lattice orientations for the asperity and substrate to make the contact incommensurate, with the details shown in SM Table S1 [34].

All simulations were performed using the open-source code LAMMPS [35]. A fixed vertical loading (N) is applied per atom in the top layer of the asperity (i.e., the group of magenta atoms shown in Fig. 1). A constant velocity $v = 1.0$ Å/ps is applied on both the magenta and orange atoms along the x direction. To mimic realistic conditions in AFM wear experiments, there is no constraint applied on the displacement in the y direction. This allows the tip to rotate and avoids severe bending stresses at the interface between the tip and the top fix boundary. The system temperature is tuned to 300 K by applying a Langevin thermostat (with the damping parameter equal to 0.05 fs) [36] in a microcanonical (*NVE*) ensemble on an additional top layer (see Fig. S2). The atomic interaction is described with the embedded-atom method (EAM) potential tabulated by Mendelev *et al.* [37], while the interfacial adhesion is tuned with the reduced Lennard-Jones (LJ) potential depth ε_{adh} (see SM Table S2 [34]). Specifically, the original well depth of the bulk LJ potential is $\varepsilon_0 = 0.70641$ eV [38], and thus the adhesion can be characterized by the parameter $\varepsilon_{adh}/\varepsilon_0$. The dislocation extraction algorithm (DXA) [39] is employed to capture the activation of plasticity. Using the shear strain and deformation gradient to calculate wear volume, as shown in SM Fig. S2 [34], these quantities enable the *in situ* and accurate measurement of wear volume. The normal and
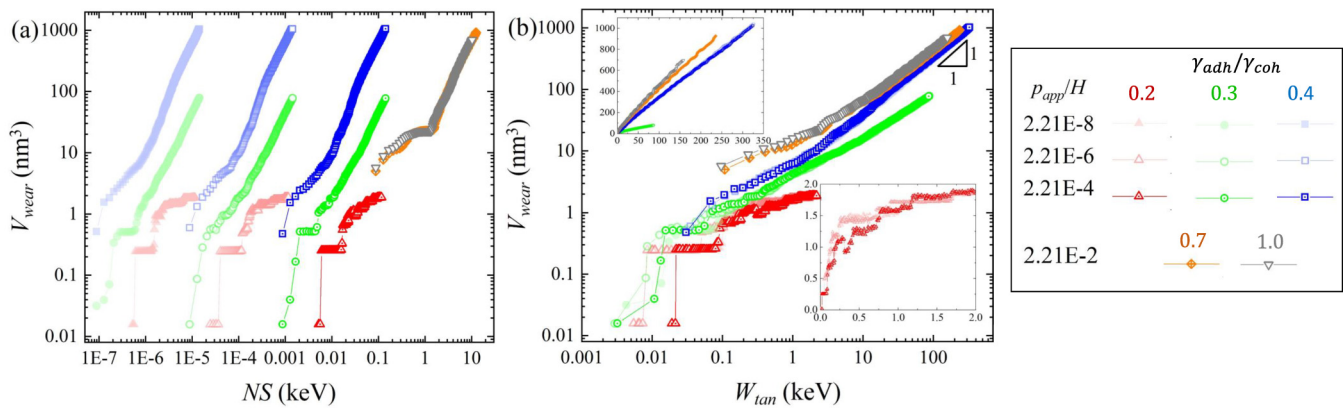
FIG. 2. Wear simulation results under different adhesions ($\varepsilon_{\mathrm{adh}}/\varepsilon_0 = 0.2$–$1.0$) and applied loads ($p_{\mathrm{app}}/H = 2.21 \times 10^{-8}$, 2.21×10^{-6}, and 2.21×10^{-4}, where H is the indentation hardness of bcc Fe [42]). Results are analyzed based on (a) the Archard-type and (b) the Reye-type wear representations. Panel (a) shows that a unique linear wear relation cannot be recovered at the single-asperity level using the Archard-type relation. Alternatively, the Rye-type representation (b) shows a linear correlation between the wear volume and the tangential work in simulations with $\varepsilon_{\mathrm{adh}}/\varepsilon_0 > 0.3$. In this regime a linear wear relation can be obtained independent of the magnitude of the applied load.

tangential forces [40] are recorded for the postanalysis. The atomic configuration is visualized using OVITO software [41].

III. RESULTS AND DISCUSSION

Wear relation at the asperity level. One of the major discussions in the community of tribology over the past decades is whether Archard's law is valid at the single-asperity level [2–4,18]. As shown in Fig. 2(a), Archard's linear correlation between wear volume (V_{wear}) and the product of loading force (N) and sliding distance (S) cannot be recovered using a fixed wear coefficient. In the lower regime of adhesion ($\varepsilon_{\mathrm{adh}}/\varepsilon_0 \Leftarrow 0.2$), no material detachment occurs within the simulation time, independent of the applied load magnitude. The negligible wear volume shown in Figs. 2(a) and 2(b) represents the minute defected atoms at the asperity tip. This observation is consistent with the ultralow wear regime observed in previous AFM experiments [2,3], where the thermally assisted atomic detachment occurs stochastically during sliding.

Inspired by our previous study [26,43], we examine the correlation between the wear volume and the tangential work, i.e., Reye's wear relation in Fig. 2(b). It can be seen that for simulations with adhesion parameter $\varepsilon_{\mathrm{adh}}/\varepsilon_0 >= 0.4$, wear curves collapse into a single curve for each adhesion parameter independent of the magnitude of the applied load. However, the wear relation in the low-adhesion regime ($\varepsilon_{\mathrm{adh}}/\varepsilon_0 < 0.4$) cannot be described with Reye's relation. This can be attributed to the fact that in the presence of a weak adhesion, the tangential work is dominantly dissipated via frictional sliding rather than plastic deformation at the asperity tip [see Fig. 1(a)]. The insets of figure Fig. 1 demonstrate qualitatively the degree of damage at the asperity tip. It can be seen that in the presence of a strong interfacial adhesion, the asperity tip undergoes severe plastic deformation.

The influence of adhesion on the wear relation. To examine Reye's wear relation, Fig. 3(a) examines the linearity of the wear relation $V_{\mathrm{wear}}/V_a \sim (W_{\mathrm{tan}}/V_a \tau_b)^\alpha$ as a function of interfacial adhesion by presenting the exponent α as a degree of linearity, where V_a is the atomic volume. Two contact regimes can be distinguished: I. the slipping regime

($\varepsilon_{\mathrm{adh}}/\varepsilon_0 =< 0.2$), where no material detachment is observed within the simulation time, and II. the adhesive wear regime ($\varepsilon_{\mathrm{adh}}/\varepsilon_0 \geqslant 0.4$), where a linear wear relation (i.e., $\alpha \sim 1$)
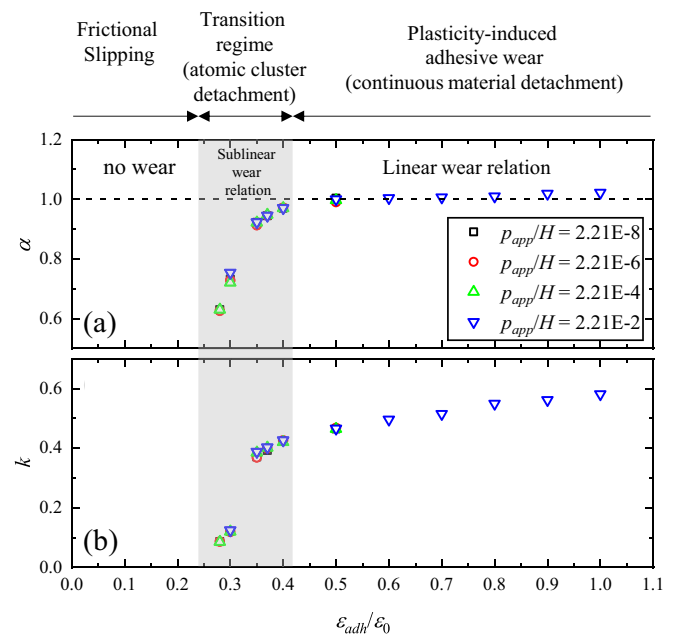

FIG. 3. (a) The wear relation exponent (α) as a function of interfacial adhesion by fitting an exponential wear model $V_{\mathrm{wear}}/V_a \sim (W_{\mathrm{tan}}/V_a \tau_b)^\alpha$. (b) Reye's wear coefficient by fitting $V_{\mathrm{wear}} = k(W_{\mathrm{tan}}/\tau_b)$. Continuous frictional slipping without material detachment is observed within the simulation time in simulations with an adhesion parameter, $\varepsilon_{\mathrm{adh}}/\varepsilon_0 < 0.2$. Simulations with an adhesion parameter $\varepsilon_{\mathrm{adh}}/\varepsilon_0 > 0.4$ show continuous material detachment in which the Reye's linear wear relation with a load-independent wear coefficient k can be obtained. The wear coefficient k increases slowly with the adhesion parameter. In the transition regime ($0.2 < \varepsilon_{\mathrm{adh}}/\varepsilon_0 < 0.4$) the correlation between the wear volume and the tangential work gradually changes from sublinear to linear ($\alpha \to 1$), where a transition from frictional slipping [Fig. 1(a)] to continuous material detachment [Fig. 1(b)] is expected.

with a load-independent wear coefficient can be obtained. There exists a transition regime from frictional slipping to material detachment where the wear relation is sublinear ($\alpha <$ 1). The wear relation becomes linear ($\alpha = 1$) when a strong interfacial adhesion presents to promote bulk plasticity at the asperity tip.

Inspired by Archard's law, we rewrite Reye's relation as $V_{\mathrm{wear}} = kW_{\mathrm{tan}}/\tau_b$ [26], where τ_b is the bulk shear strength ($\sim$21.6 GPa for bcc Fe at 300 K [44]) and k is Reye's wear coefficient. The wear coefficient of k in Reye's relation presents the fraction of frictional work dissipated by bulk plasticity (i.e., the efficiency of plasticity-induced material detachment). Figure 3(b) shows that the Reye's wear coefficient increases with adhesion, corresponding to the wear regimes defined in Fig. 3(a). It should be emphasized that to obtain the Reye's wear coefficient for nonlinear curves (i.e., $\alpha < 1$) the fitting procedure is carried out only for the linear range of data [see Fig. 2(b)].

The transition from a sublinear to linear wear relation can be understood from the mechanism of material detachment from the tip. Inspired by the Archard's assumption [26], which was recently confirmed by numerical simulations [25], we hypothesize that a linear wear relation can only be recovered when the material detachment from the asperity tip is dominated by bulk plasticity. Depending on materials and contact conditions, various plasticity mechanisms can be present at the asperity tip, e.g., dislocation plasticity [45–47], amorphization [48,49], and grain-boundary-mediated plasticity [50,51].

Fig. 4 shows dislocations activity at the contact interface as a function of sliding distance. In the low-adhesion regime ($\varepsilon_{\mathrm{adh}}/\varepsilon_0 < 0.2$), the tangential work is mainly dissipated at the contact by frictional slipping, where only misfit dislocations are present at the contact interface between the tip and the substrate due to the crystalline lattice mismatch [Fig. 4(a1)]. While a small degree of atomic rearrangement occurs at the contact interface, the lattice structure in the asperity tip remains unchanged during frictional slipping. Under this condition, no bulk (i.e., volumetric) dislocation plasticity and material detachment can be observed.

In the transitional regime ($\varepsilon_{\mathrm{adh}}/\varepsilon_0 = 0.2 - 0.4$), while only misfit dislocations are present at the contact interface [Fig. 4(a2)], a larger degree of atomic rearrangement (i.e., interfacial amorphization) occurs at the asperity tip. As a result, minute atomic clusters occasionally detach due to local thermal-induced atomic vibrations at the contact (i.e., atomic attrition [2,3]). In this regime, a sublinear wear relation (e.g., Arrhenius-type equation) may be expected [52]. The linear correlation between the dislocation length and the contact size [Fig. 4(c)], which is consistent with the theoretical explanation of sliding friction [53], confirms the solitary presence of misfit dislocations at the contact between the tip and the rigid substrate.

Alternatively, in the high-adhesion regime ($\varepsilon_{\mathrm{adh}}/\varepsilon_0 > 0.4$), interfacial dislocations presented at the contact migrate into the bulk [Fig. 4(a3)], causing volumetric plasticity at the asperity tip (i.e., dislocation-mediated interface migration). In other words, the contact interface between the asperity and the rigid substrate turns into a grainlike boundary in the asperity tip. As shown, atoms at both sides of the boundary rearrange

to a minimum energy configuration, causing an initial drop in the total dislocations length [see Fig. 4(b)]. As shown in Fig. 4(a3) [see also Fig. 1(c)], the crystal orientation of detached material from the asperity tip acquires the orientation of the substrate. Upon sliding, the tangential stress at the contact causes further migration of the boundary into the bulk, causing as increase in the boundary area and the total dislocation length.

The horizontal displacement of the asperity in the high-adhesion regime is accommodated by dislocation glide on slip planes in the bulk instead of the original contact interface. A linear correlation between the wear volume and the tangential work can be understood, as the tangential work mainly dissipates by volumetric (bulk) plasticity, where frictional slipping is suppressed due to a strong interfacial adhesion. In this case, the plastically deformed volume of the tip pastes over the substrate and a linear wear relation is recovered. It is worth mentioning that Fe is chosen as a model material in this study; therefore one should expect similar wear mechanisms and regimes with other ductile metallic systems. It has been discussed that [57–62] the contact size at the asperity level controls the behavior of dislocations at the contact interface. The movement of dislocation from the contact plane to the asperity bulk, which is observed in this study, can be a direct result of dislocation trapping at the contact [57,58]. Further studies are needed to explore the effect of the contact geometry (e.g., the asperity size and shape) [8,63] and chemical conditions [55] at the interface on the transition in wear mechanisms. It would be also interesting to study the case of asperity sliding over a deformable substrate [64,65], where a larger degree of atomic rearrangement at the contact interface may further trigger dislocation movement into the asperity bulk.

In AFM adhesive wear experiments [2–4], the degree of chemical solubility and material passivation as well as the tip surface roughness governs the degree of interfacial adhesion and corresponding wear mechanism. Increasing the normal load and the contact temperature favors a linear relation between the wear volume and tangential work. Additionally, lateral interactions between interlocking asperities, which to a large extent presents at the contact between rough surfaces, further suppress the frictional slipping mechanism and promote plasticity-induced material detachment. This may explain the widely observed linear wear relation in macroscopic wear experiments in particular for metallic materials, where plastic deformation play a central role at the contact. It is yet of interest to study the effect of elastic and plastic interaction between neighboring asperities in multiasperity contact on the material detachment mechanisms and wear relation.

IV. CONCLUSION

In summary, large-scale MD simulations are performed to study the adhesive wear behavior at the single-asperity level. Consistent with previous AFM experiments and numerical simulations, our results show that the Archard's wear relation fails to characterize wear behavior at the single-asperity level, particularly in the presence of a low interfacial adhesion and applied normal load. Alternatively, our simulations show that a linear wear relation can be recovered via the Reye's wear
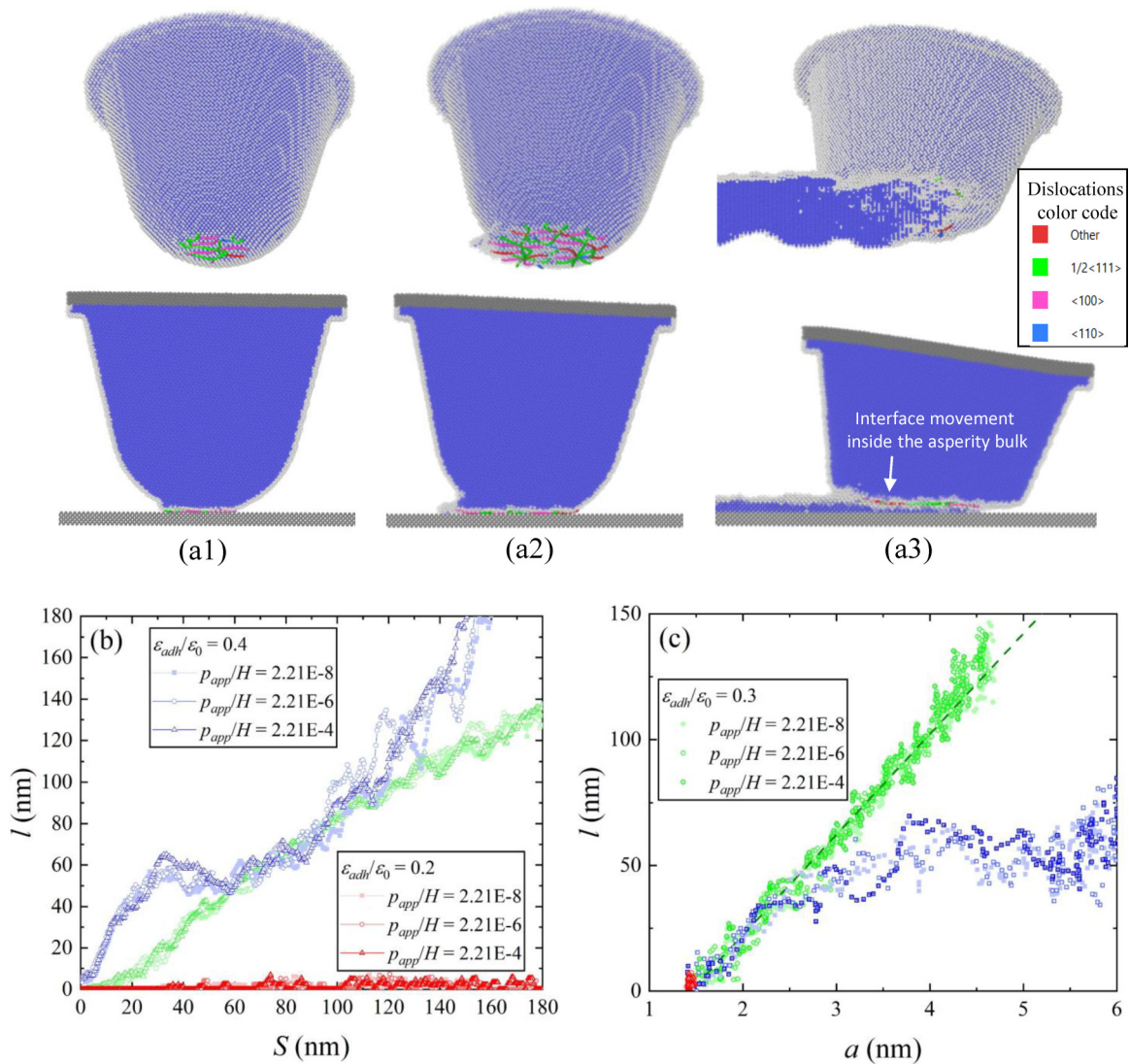
FIG. 4. (a) Visualization of dislocations activity at the contact between the tip and the substrate in simulations with the adhesion parameter $\varepsilon_{adh}/\varepsilon_0$(a1) = 0.2, (a2) = 0.3, and (a3) = 0.4 under applied load $p_{app}/H = 2.21 \times 10^{-6}$. The substrate has been omitted from the snapshot for clarity. The blue atoms are of bcc structure, while the white ones are amorphous. Dislocations are identified by the DXA algorithm. While dislocations remain at the contact in the first two cases ($\varepsilon_{adh}/\varepsilon_0 = 0.2$ and 0.3), they migrate into the asperity bulk, forming a grain-boundary-like interface in the asperity tip for $\varepsilon_{adh}/\varepsilon_0 = 0.4$. See Supplemental Material, Movies 2 and 3 [34] for more information. (b) Evolution of total dislocation length (l) as a function of sliding distance (S) for different adhesion cases. (c) Dislocation length (l) vs contact size (a). See Supplemental Material, Fig. S3 [34] for detailed measurement of contact size, which is consistent with JKR [54–56] prediction before sliding. It can be seen that the dislocation line is proportional to the contact size when frictional slipping is dominant.

relation only if the material removal is dominantly progressed by bulk plasticity. This observation confirms Archard's theoretical argument that the only possible mechanism to recover a linear wear relation at the asperity level is the removal of lumps from contact areas formed by plastic deformation.

Additionally, it is shown that the interfacial adhesion dictates the mechanism of wear and transition from a discrete to continuous material detachment. At the low-adhesion regime, the work of tangential force mainly dissipates through frictional slipping through the movement of misfit dislocations in the contact. Thermally assisted atomic cluster detachment may present during frictional sliding. In the presence of strong adhesion, bulk plasticity occurs at the asperity tip, causing the detachment of material from the asperity tip. Under this condition, a linear correlation between the tangential work and wear volume can be recovered, where the coefficient represents the fraction of frictional work dissipated by bulk plasticity.

ACKNOWLEDGMENTS

[1] B. Bhushan, *Modern Tribology Handbook* (CRC Press, Boca Raton, FL, 2000).

[2] T. D. B. Jacobs and R. W. Carpick, Nanoscale wear as a stress-assisted chemical reaction, Nat. Nanotechnol. **8**, 108 (2013).

[3] H. Bhaskaran, B. Gotsmann, A. Sebastian, U. Drechsler, M. A. Lantz, M. Despont, P. Jaroenapibal, R. W. Carpick, Y. Chen, and K. Sridharan, Ultralow nanoscale wear through atom-by-atom attrition in silicon-containing diamond-like carbon, Nat. Nanotechnol. **5**, 181 (2010).

[4] B. Gotsmann and M. A. Lantz, Atomistic Wear in a Single Asperity Sliding Contact, Phys. Rev. Lett. **101**, 125501 (2008).

[5] B. N. J. Persson, Contact mechanics for randomly rough surfaces, Surf. Sci. Rep. **61**, 201 (2006).

[6] B. N. J. Persson and E. Tosatti, The effect of surface roughness on the adhesion of elastic solids, J. Chem. Phys. **115**, 5597 (2001).

[7] B. N. J. Persson, Elastoplastic Contact between Randomly Rough Surfaces, Phys. Rev. Lett. **87**, 116101 (2001).

[8] E. Milanese, T. Brink, R. Aghababaei, and J.-F. Molinari, Emergence of self-affine surfaces during adhesive wear, Nat. Commun. **10**, 1116 (2019).

[9] J. A. Greenwood and J. B. Williamson, Contact of nominally flat surfaces, Proc. R. Soc. London A **295**, 300 (1966).

[10] A. Schirmeisen, One atom after the other, Nat. Nanotechnol. **8**, 81 (2013).

[11] F. P. Bowden and D. Tabor, *The Friction and Lubrication of Solids* (Clarendon Press, Oxford, 2001).

[12] J. F. Archard, Contact and rubbing of flat surfaces, J. Appl. Phys. **24**, 981 (1953).

[13] J. T. Burwell and C. D. Strang, On the empirical law of adhesive wear, J. Appl. Phys. **23**, 18 (1952).

[14] F. J. Giessibl, Atomic resolution of the silicon (111)-(7 × 7) surface by atomic force microscopy, Science **267**, 68 (1995).

[15] R. W. Carpick and M. Salmeron, Scratching the surface: Fundamental investigations of tribology with atomic force microscopy, Chem. Rev. **97**, 1163 (1997).

[16] S. Izabela, C. Michael, and W. C. Robert, Recent advances in single-asperity nanotribology, J. Phys. D Appl. Phys. **41**, 123001 (2008).

[17] R. Agrawal, N. Moldovan, and H. D. Espinosa, An energy-based model to predict wear in nanocrystalline diamond atomic force microscopy tips, J. Appl. Phys. **106**, 064311 (2009).

[18] Z. D. Sha, V. Sorkin, P. S. Branicio, Q. X. Pei, Y. W. Zhang, and D. J. Srolovitz, Large-scale molecular dynamics simulations of wear in diamond-like carbon at the nanoscale, Appl. Phys. Lett. **103**, 073118 (2013).

[19] J. Liu, J. K. Notbohm, R. W. Carpick, and K. T. Turner, Method for characterizing nanoscale wear of atomic force microscope tips, ACS Nano **4**, 3763 (2010).

[20] K.-H. Chung, Y.-H. Lee, and D.-E. Kim, Characteristics of fracture during the approach process and wear mechanism of a silicon AFM tip, Ultramicroscopy **102**, 161 (2005).

[21] R. Aghababaei, On the origins of third-body particle formation during adhesive wear, Wear **426–427**, 1076 (2019).

[22] A. R. Hinkle, W. G. Nöhring, R. Leute, T. Junge, and L. Pastewka, The emergence of small-scale self-affine surface roughness from deformation, Sci. Adv. **6**, eaax0847 (2020).

[23] R. Aghababaei, D. H. Warner, and J. F. Molinari, Critical length scale controls adhesive wear mechanisms, Nat. Commun. **7**, 11816 (2016).

[24] R. Aghababaei, Effect of adhesion on material removal during adhesive wear, Phys. Rev. Mater. **3**, 063604 (2019).

[25] R. Aghababaei, T. Brink, and J.-F. Molinari, Asperity-Level Origins of Transition from Mild to Severe Wear, Phys. Rev. Lett. **120**, 186105 (2018).

[26] R. Aghababaei, D. H. Warner, and J. F. Molinari, On the debris-level origins of adhesive wear, Proc. Natl. Acad. Sci. USA **114**, 7935 (2017).

[27] T. Reye, Zur theorie der zapfenreibung, Civilingenieur **4**, 235 (1860).

[28] G. Fleischer, H. Gröger, and H. Thum, *Verschleiß und Zuverlässigkeit* (Verlag Technik, 1980).

[29] H. Uetz and J. Fohl, Wear as an energy transformation process, Wear **49**, 253 (1978).

[30] E. Rabinowicz, *Friction and Wear of Materials* (Wiley, New York, 1965).

[31] E. J. W. Whittaker, Friction and wear, Nature (London) **159**, 541 (1947).

[32] Y. Mo, K. T. Turner, and I. Szlufarska, Friction laws at the nanoscale, Nature (London) **457**, 1116 (2009).

[33] Y. F. Mo and I. Szlufarska, Roughness picture of friction in dry nanoscale contacts, Phys. Rev. B **81**, 035405 (2010).

[34] See Supplemental Material at http://link.aps.org/supplemental/10.1103/PhysRevMaterials.4.103605 for complementary figures, tables, and description of wear volume measurements.

[35] S. Plimpton, Fast parallel algorithms for short-range molecular dynamics, J. Comput. Phys. **117**, 1 (1995).

[36] T. Schneider and E. Stoll, Molecular-dynamics study of a three-dimensional one-component model for distortive phase transitions, Phys. Rev. B **17**, 1302 (1978).

[37] M. I. Mendelev, S. Han, D. J. Srolovitz, G. J. Ackland, D. Y. Sun, and M. Asta, Development of new interatomic potentials appropriate for crystalline and liquid iron, Philos. Mag. **83**, 3977 (2003).

[38] V. P. Filippova, E. N. Blinova, and N. A. Shurygina, Constructing the pair interaction potentials of iron atoms with other metals, Inorg. Mater. Appl. Res. **6**, 402 (2015).

[39] A. Stukowski, V. V. Bulatov, and A. Arsenlis, Automated identification and indexing of dislocations in crystal interfaces, Model. Simul. Mater. Sci. Eng. **20**, 085007 (2012).

[40] S. Bogusz, T. E. Cheatham, and B. R. Brooks, Removal of pressure and free energy artifacts in charged periodic systems via net charge corrections to the Ewald potential, J. Chem. Phys. **108**, 7070 (1998).

[41] A. Stukowski, Visualization and analysis of atomistic simulation data with OVITO—The Open Visualization Tool, Model. Simul. Mater. Sci. Eng. **18**, 015012 (2010).

[42] K. Zhao, A. E. Mayer, J. Y. He, and Z. L. Zhang, Dislocation based plasticity in the case of nanoindentation, Int. J. Mech. Sci. **148**, 158 (2018).

[43] K. Zhao and R. Aghababaei, Adhesive wear law at the single asperity level, J. Mech. Phys. Solids **143**, 104069 (2020).

[44] F. T. Latypov and A. E. Mayer, Shear strength of metals under uniaxial deformation and pure shear, J. Phys.: Conf. Ser. **653**, 012041 (2015).

[45] A. Moshkovich, V. Perfilyev, I. Lapsker, and L. Rapoport, Friction, wear and plastic deformation of Cu and α/β brass under lubrication conditions, Wear **320**, 34 (2014).

[46] R. A. Bernal and R. W. Carpick, Visualization of nanoscale wear mechanisms in ultrananocrystalline diamond by in-situ TEM tribometry, Carbon **154**, 132 (2019).

[47] D. Sagapuram, K. Viswanathan, A. Mahato, N. K. Sundaram, R. M'Saoubi, K. P. Trumble, and S. Chandrasekar, Geometric flow control of shear bands by suppression of viscous sliding, Proc. R. Soc. London, Ser. A **472**, 20160167 (2016).

[48] X. L. Hu, M. V. P. Altoe, and A. Martini, Amorphization-assisted nanoscale wear during the running-in process, Wear **370**, 46 (2017).

[49] L. Pastewka, S. Moser, P. Gumbsch, and M. Moseler, Anisotropic mechanical amorphization drives wear in diamond, Nat. Mater. **10**, 34 (2011).

[50] H. A. Padilla, B. L. Boyce, C. C. Battaile, and S. V. Prasad, Frictional performance and near-surface evolution of nanocrystalline Ni-Fe as governed by contact stress and sliding velocity, Wear **297**, 860 (2013).

[51] J. W. Cahn, Y. Mishin, and A. Suzuki, Coupling grain boundary motion to shear deformation, Acta Mater. **54**, 4953 (2006).

[52] J. Liu, Y. Jiang, D. S. Grierson, K. Sridharan, Y. Shao, T. D. B. Jacobs, M. L. Falk, R. W. Carpick, and K. T. Turner, Tribochemical Wear of Diamond-Like Carbon-Coated Atomic Force Microscope Tips, ACS Appl. Mater. Interfaces **9**, 35341 (2017).

[53] Z. W. Gao, W. Zhang, and Y. F. Gao, Scale dependence of interface dislocation storage governing the frictional sliding of single asperities, Model. Simul. Mater. Sci. Eng. **24**, 065010 (2016).

[54] K. L. Johnson, K. Kendall, and A. D. Roberts, Surface energy and the contact of elastic solids, Proc. R. Soc. Lond. A **324**, 301 (1971).

[55] R. W. Carpick, N. Agrait, D. F. Ogletree, and M. Salmeron, Variation of the interfacial shear strength and adhesion of a nanometer-sized contact, Langmuir **12**, 3334 (1996).

[56] S. B. Vishnubhotla, R. Chen, S. R. Khanal, A. Martini, and T. D. B. Jacobs, Understanding contact between platinum nanocontacts at low loads: The effect of reversible plasticity, Nanotechnology **30**, 035704 (2019).

[57] J. A. Hurtado and K. S. Kim, Scale effects in friction of single-asperity contacts, I. From concurrent slip to single-dislocation-assisted slip, Proc. R. Soc. London, Ser. A **455**, 3363 (1999).

[58] J. A. Hurtado and K. S. Kim, Scale effects in friction of single-asperity contacts, II. Multiple-dislocation-cooperated slip, Proc. R. Soc. London, Ser. A **455**, 3385 (1999).

[59] Y. Gao, A Peierls perspective on mechanisms of atomic friction, J. Mech. Phys. Solids **58**, 2023 (2010).

[60] T. A. Sharp, L. Pastewka, V. L. Ligneres, and M. O. Robbins, Scale- and load-dependent friction in commensurate sphere-on-flat contacts, Phys. Rev. B **96**, 155436 (2017).

[61] T. A. Sharp, L. Pastewka, and M. O. Robbins, Elasticity limits structural superlubricity in large contacts, Phys. Rev. B **93**, 121402 (2016).

[62] V. S. Deshpande, A. Needleman, and E. Van der Giessen, Discrete dislocation plasticity analysis of static friction, Acta Mater. **52**, 3135 (2004).

[63] L. Pei, S. Hyun, J. F. Molinari, and M. O. Robbins, Finite element modeling of elasto-plastic contact between rough surfaces, J. Mech. Phys. Solids **53**, 2385 (2005).

[64] J. Zhong, R. Shakiba, and J. B. Adams, Molecular dynamics simulation of severe adhesive wear on a rough aluminum substrate, J. Phys. D Appl. Phys. **46**, 055307 (2013).

[65] B. W. Ewers and J. D. Batteas, The role of substrate interactions in the modification of surface forces by self-assembled monolayers, RSC Adv. **4**, 16803 (2014).